RECENT RESULTS FROM THE CMD-2 DETECTOR AT VEPP-2M COLLIDER

R.R.AKHMETSHIN, G.A.AKSENOV, E.V.ANASHKIN, M.ARPAGAUS, V.A.ASTAKHOV, V.M.AULCHENKO, B.O.BAIBUSINOV, V.S.BANZAROV, L.M.BARKOV, S.E.BARU, A.E.BONDAR, D.V.CHERNYAK, V.V.DANILOV, S.I.EIDELMAN, G.V.FEDOTOVICH, N.I.GABYSHEV, A.A.GREBENIUK, D.N.GRIGORIEV, B.I.KHAZIN, I.A.KOOP, A.S.KUZMIN, M.LECHNER, I.B.LOGASHENKO, P.A.LUKIN, A.P.LYSENKO, A.V.MAKSIMOV, Yu.I.MERZLYAKOV, I.N.NESTERENKO, V.S.OKHAPKIN, E.A.PEREVEDENTSEV, A.A.POLUNIN, E.V.POPKOV, V.I.PTITZYN, T.A.PURLATZ, S.I.REDIN, N.I.ROOT, A.A.RUBAN, N.M.RYSKULOV, Yu.M.SHATUNOV, M.A.SHUBIN, B.A.SHWARTZ, V.A.SIDOROV, A.N.SKRINSKY, V.P.SMAKHTIN, I.G.SNOPKOV, E.P.SOLODOV, A.I.SUKHANOV, V.M.TITOV, Yu.V.YUDIN, V.G.ZAVARZIN

Budker Institute of Nuclear Physics, Novosibirsk, 630090, Russia

D.H.BROWN, J.P.MILLER, B.L.ROBERTS, W.A.WORSTELL

Boston University, Boston, MA 02215, USA

J.A.THOMPSON, C.M.VALINE

University of Pittsburgh, Pittsburgh, PA 15260, USA

P.B.CUSHMAN

University of Minnesota, Minneapolis, Minnesota 55455, USA

S.K.DHAWAN, V.W.HUGHES

Yale University, New Haven, CT 06511, USA

The general purpose detector CMD-2 is taking data at the e^+e^- collider VEPP-2M at Novosibirsk in the energy range 360 -1400 MeV. The integrated luminosity $\approx 4000nb^{-1}$ of around ϕ meson mass (5.0×10^6 *of* ϕ's) and $\approx 500nb^{-1}$ in the 600-1000 MeV range have been collected. A latest analysis of the rare decays of ϕ meson based on 30% of available data is presented in this paper. Data from the 600 - 1000 MeV energy range are used for high accuracy measurements of the e^+e^- annihilation cross section into hadrons and measurements of the ω meson parameters. A preliminary analysis for the electron width and full width of ω meson is presented.

1 Introduction

1.1 VEPP-2M collider

The VEPP-2M collider [1] at the Budker Institute of Nuclear Physics in Novosibirsk, Russia, covers the center of mass energy range from the two pion threshold up to 1400 MeV. Experiments at this collider yielded a number of important results in e^+e^- physics, including the most precise pion form factor measurements [2] and studies of the ϕ, ω, and ρ meson decays [3,4]. During 1988-92 a new booster was installed to allow higher positron current and with 40 mA per beam VEPP-2M has peak luminosity $L \approx 5. \times 10^{30} cm^{-2}s^{-1}$ at the ϕ center of mass energy.

1.2 CMD-2 detector

The CMD-2 detector has been described in more detail elsewhere [5–7].

The data with the luminosity integral $\approx 300nb^{-1}$ collected in 1992-1993 at ϕ were used for the measurement of ϕ meson parameters and branching ratios into four major decay modes [7].

The integrated luminosity $\approx 1500nb^{-1}$ around ϕ mass has been collected during the 1993 summer

run and was used for studies of rare decay modes of ϕ, coupled $K_S K_L$ decays and nuclear interactions of neutral kaons. Some preliminary results are published in [8] and in this paper we present latest analysis based on 1992-1993 data.

The 1994-1995 runs were dedicated mostly to measurements of the total hadronic cross section at the energies below ϕ resonance [9] where the integrated luminosity about $500nb^{-1}$ has been collected. In this paper we present preliminary results on ω meson parameters measurement based on 122 nb^{-1} collected around ω peak.

Additional 2000 nb^{-1} have been collected around ϕ peak in 1996 spring run and these data are under analysis now.

2 Rare ϕ decays study

2.1 $\phi \to \eta\gamma$ and $\phi \to \eta'\gamma$

The decay $\phi \to \eta\gamma$ was previously observed in neutral modes ($\eta \to \gamma\gamma$, $\eta \to 3\pi^0$) only. Detector CMD-2 gives the possibility to study $\phi \to \eta\gamma$ decay in the channel with charged particles, when η decays into $\pi^+\pi^-\pi^0$. The primary photon has the highest energy of all three in the final state - 362 MeV at the ϕ meson peak and was required be detected in events selection.

The reconstructed invariant mass of 3 pions $M_{\pi^+\pi^-\pi^0}$ was used to select the decay $\phi \to \eta\gamma$ and the distribution over it had a peak around M_η = 547.45 MeV. After background subtraction 1100±40 events were selected.

The experimental cross section $\sigma(e^+e^- \to \phi \to \eta\gamma)$ with a fit function is presented in Figure 1. The obtained parameters of ϕ meson M_ϕ=1019.31±0.18 MeV and Γ_ϕ=4.70±0.25 MeV are in good agreement with table values[10]. Using the electron width of ϕ from [10] the $Br(\phi \to \eta\gamma)$ was found to be:

$$Br(\phi \to \eta\gamma) = (1.29 \pm 0.07) \times 10^{-2}.$$

The decay $\phi \to \eta'\gamma$ was searched in the mode, when η' decays into $\pi^+\pi^-\eta$ and $\eta \to \gamma\gamma$. So, both $\eta\gamma$ and $\eta'\gamma$ final states have 2 charged particles and 3 photons. The events with all these particles detected were used for the constrained fit and as a result 481 events of $\eta\gamma$ were selected.

The decay into $\eta\gamma$ is the basic background for the $\eta'\gamma$ search and after anti-$\eta\gamma$ cut the scatter

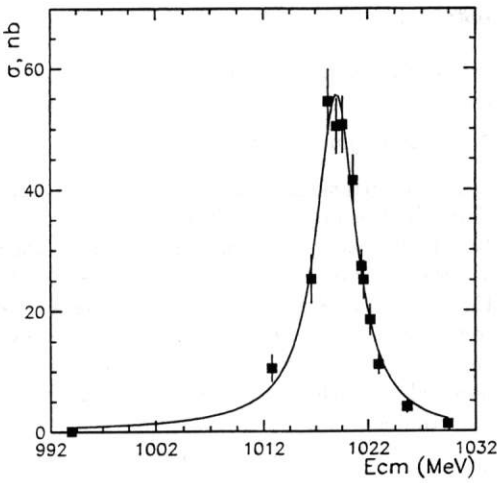

Figure 1: The $\phi \to \eta\gamma$ cross-section.

plot of the invariant mass of two hardest photons M_{12} versus the weakest photon energy ω_3 was studied. For $\eta'\gamma$ events M_{12} should be close to η mass 547.5 MeV, while ω_3 is a monochromatic 60 MeV photon. The Figure 2 presents the re-

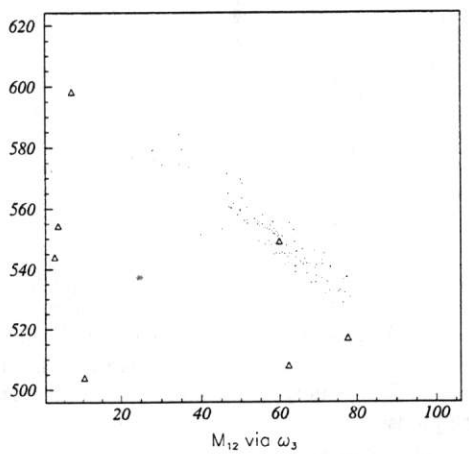

Figure 2: Invariant mass M_{12}(MeV) vs. ω_3(MeV) after constrained fit. Dots are simulation, triangles - experiment.

sult of 1992–1993 data together with simulation of $\phi \to \eta'\gamma$. We have 1 candidate to $\eta'\gamma$ event with 1 event as estimated background. Using for the 90% C.L. upper limit $N_{\eta'\gamma}$ <3 and the efficiencies obtained from the simulation, $\varepsilon_{\eta\gamma}$ = 14.4% and $\varepsilon_{\eta'\gamma}$ = 6.4%, the following result has been

obtained:

$$Br(\phi \to \eta'\gamma) \ < \ 2.4 \cdot 10^{-4}.$$

2.2 Search for $\phi \to \pi^+\pi^-\pi^+\pi^-$

A 3- and 4-tracks events were selected as a candidates for the process $\phi \to \pi^+\pi^-\pi^+\pi^-$. But due to a high background from the main channels of ϕ decaying into 3-tracks events, in the search for the process $\phi \to \pi^+\pi^-\pi^+\pi^-$ only 4-tracks events were used. The ratio of 3- and 4-tracks events at the energy points outside the ϕ meson region was used (along with a simulation) for evaluation of a detection efficiency.

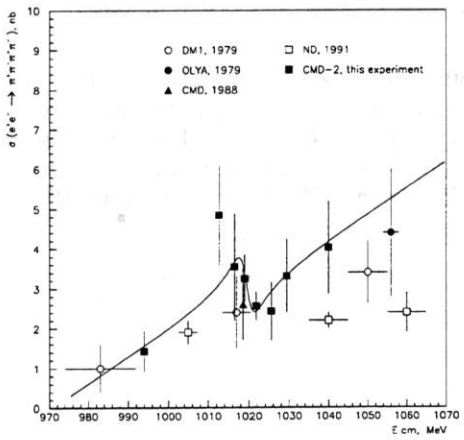

Figure 3: The cross-section $e^+e^- \to \pi^+\pi^-\pi^+\pi^-$.

To extract the number of events of the process $e^+e^- \to \pi^+\pi^-\pi^+\pi^-$ we apply a simple cut to the total momentum of 4 charged particles (should be around zero) and their total energy (should be arounf $E_{c.m.}$ energy), assuming that all particles are pions.

The cross-section vs. energy for the process $e^+e^- \to \pi^+\pi^-\pi^+\pi^-$ is shown in Figure 3. Only statistical errors are shown. A function which describes interference of linear background with the amplitude of the process $\phi \to \pi^+\pi^-\pi^+\pi^-$ was used for the fitting taking into account only this experiment. The result of the fit is shown in the plot by a smooth line. Using this fit and the uncertainty in the efficiency, one can get

$$Br(\phi \to \pi^+\pi^-\pi^+\pi^-) < 1. \times 10^{-4}, \ 90\% \text{ C.L.}$$

2.3 Search for $\phi \to f_0(980)\gamma$

The event candidates were selected by a requirement of two charged tracks in the DC and one or two photons with energy greater than 20 MeV in the CsI calorimeter. All particles were required to be in the polar angle between 0.85 and 2.25 radians for the bremsstrahlung processes suppression. The sum of the energy depositions of two clusters associated with the charged tracks was required to be less than 450 MeV to remove Bhabha events.

The main background for the studied process was $\phi \to \pi^+\pi^-\pi^0$ decay when one of the gamma from π^0 escaped detection. To reduce this background a constrained fit was used. The rest of the 3π background was removed by selection of gamma energy in the range 20 MeV< E_γ <100 MeV, where signal of f_0 was expected. The muon range system was used to remove $\mu^+\mu^-\gamma$ contamination.

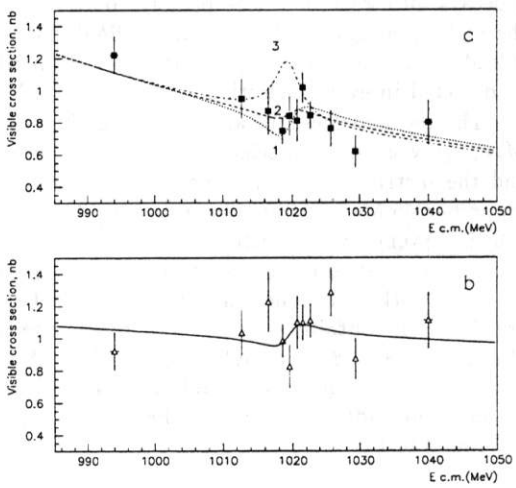

Figure 4: a. Visible cross section for $e^+e^- \to \pi^+\pi^-\gamma$. Lines are theoretical predictions in case of no $f_0\gamma$ signal (2), $f_0\gamma$ signal with B($\phi \to f_0\gamma$)=2.4×10^{-4} for negative relative phase (3) and positive relative phase (1); b. Visible cross section for $e^+e^- \to \mu^+\mu^-\gamma$ with theoretical prediction.

Under these conditions 833±30 events of $\pi^+\pi^-\gamma$ and 846±31 of $\mu^+\mu^-\gamma$ events were selected with the integrated luminosity of 1269 nb^{-1}, de-

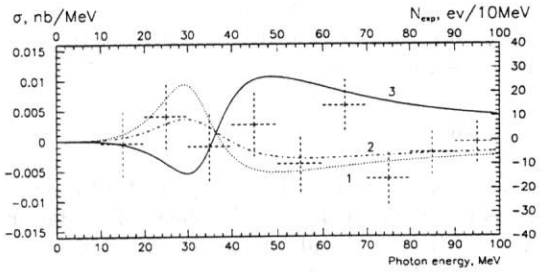

Figure 5: Difference in spectrum for gamma at "ϕ" region and "non-ϕ" region, normalized to integrated luminosity. Lines are theoretical prediction for four quark model for 2.4×10^{-4} branching ratio in case of positive(1) and negative(3) interference sign with 40 MeV f_0 width. Line (2) is for 100 MeV f_0 width.

termined by Bhabha events. The detection efficiency was found by simulation to be 17%. The experimental cross sections vs. center of mass energies are presented in figures 4a,b.

The signal from $\phi \rightarrow f_0(980)\gamma$ decay was searched as an interference paterns in the cross section vs. energy behavior of the $e^+e^- \rightarrow \pi^+\pi^-\gamma$ process and in the difference in gamma spectra of the selected events at ϕ peak and near the ϕ region. According to the theoretical calculations [11] the following interference paterns were used for $f_0\gamma$ search: a) interference of the background process $e^+e^- \rightarrow \pi^+\pi^-\gamma$ with "radiative" decay of $e^+e^- \rightarrow \phi \rightarrow \gamma \rightarrow \pi^+\pi^-\gamma$ when no f_0 present. This is valid also for $\mu^+\mu^-\gamma$ process; and b) interference of the two above processes with $e^+e^- \rightarrow \phi \rightarrow f_0\gamma \rightarrow \pi^+\pi^-\gamma$ when f_0 was described as a four quark state. The model predictions are shown in figures 4a,b for the cross section and in figures 5 for the difference in gamma spectra. Using these interference paterns the following results were obtaind at the 90% CL:
$Br(\phi \rightarrow \pi^+\pi^-\gamma) < 1.5 \times 10^{-5}$,
$Br(\phi \rightarrow \mu^+\mu^-\gamma) < 2.6 \times 10^{-5}$,
$Br(\phi \rightarrow f_0\gamma) < 7 \times 10^{-4}$.

2.4 Search for $\phi \rightarrow \eta e^+e^-$

The decay mode $\eta \rightarrow \gamma\gamma$ was chosen. The typical characteristics are the invariant mass of the two gammas (0.54 GeV), the small space angle between the two electrons and the sum of the momenta of the electrons (0.364 GeV) The main backgrounds are: a) $\phi \rightarrow \eta\gamma$ with gamma conversion in the beam pipe and b) $e^+e^- \rightarrow e^+e^-\gamma\gamma$ where the two electrons come from an internal gamma conversion. Full kinematical reconstruction was done and calibrated with $\phi \rightarrow \pi^+\pi^-\pi^0$ events at small angle between the two charged pions. The QED-process $e^+e^- \rightarrow e^+e^-\gamma$ was used to calibrate efficiency of the drift chamber for charged particles at small space angle and photon conversion probability in the beam pipe. The total luminosity was 2085 nb^{-1}, corresponding to 2,715,000 ϕ's.

In the region indicated in the figure 6 around η mass 12 events are seen and 4.2 are expected from all backgrounds. The branching ratio was found to be

$$Br(\phi \rightarrow \eta e^+e^-) = (1.10\pm\ 0.49\pm0.19)\times10^{-4}.$$

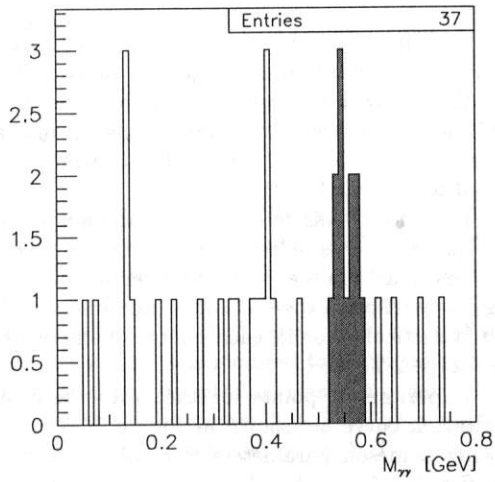

Figure 6: The invariant mass of the two photons after constraind fit

3 Measurements of ω meson parameters

The c.m. energy region from 2x380 to 2x405 MeV has been scanned at 13 energy points with a total luminosity integral of 122 nb^{-1}. The beam energy in each point has been measured by the resonant depolarization technique[12] and is known to an accuracy better than 10^{-4}.

An events with two non-collinear tracks were selected as a candidate for a $\omega \rightarrow \pi^+\pi^-\pi^0$ decay. The resulting number 13489 of $\pi^+\pi^-\pi^0$ events

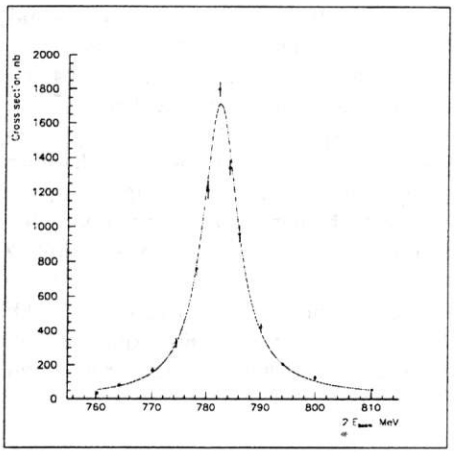

Figure 7: ω meson excitation curve.

were obtained by fitting the missing mass $M^2_{\pi^0}$ parameter histograms and background subtraction.

Events, with two detected gammas from neutral pions were used for combined trigger and reconstruction efficiency determination which was found to be 0.91 ± 0.01.

Luminosity was determined by the number of the Bhabha events, selected by the presence of two collinear tracks in the Drift Chamber and high energy deposition in the CsI barrel calorimeter with the statistical error in each energy point on the level of 1–2 %.

Experimental points together with the fitted excitation curve are shown in Figure 7. The following ω-meson parameters were obtained from the fit:
$\Gamma_{e^+e^-} = 0.62 \pm 0.01 \pm 0.02$ keV,
$\Gamma_{tot} = 8.23 \pm 0.20 \pm 0.30$ MeV.

4 Conclusion

The CMD-2 detector is taking data at the VEPP-2M collider in Novosibirsk. Data collection was performd at the ϕ meson region and at the energy range 600-1000 MeV. About 30% of available data have been analized. The new results in rare ϕ decays study
$Br(\phi \to \eta\gamma) = (1.29 \pm 0.07) \times 10^{-2}$,
$Br(\phi \to \eta'\gamma) < 2.4 \times 10^{-4}$,
$Br(\phi \to \pi^+\pi^-\pi^+\pi^-) < 1.0 \times 10^{-4}$,
$Br(\phi \to f_0\gamma) < 7 \times 10^{-4}$,
$Br(\phi \to \pi^+\pi^-\gamma) < 1.5 \times 10^{-5}$,
$Br(\phi \to \mu^+\mu^-\gamma) < 2.6 \times 10^{-5}$,
$Br(\phi \to \eta e^+e^-) = (1.10 \pm 0.49 \pm 0.19) \times 10^{-4}$
have been obtained.

Acknowledgments

This work is supported in part by the US Departament of Energy, US National Science Foundation and the International Science Foundation under grants RPT000 and RPT300.

References

1. V.V. Anashin *et al*, Preprint BudkerINP 84-114, Novosibirsk, 1984.
2. L.M. Barkov *et al*, *Nucl. Phys.* B **364**, 199 (1985).
3. A.D. Bukin *et al*, *Sov. Journal of Nucl. Phys.* **27**, 516 (1978).
4. S.I.Dolinsky *et al*, *Phys. Report* **202**, 99 (1991).
5. G.A.Aksenov *et al*, Preprint BudkerINP 85-118, Novosibirsk, 1985.
6. E.V. Anashkin *et al*, ICFA Instrumentation Bulletin 5 (1988), p.18.
7. R.R. Akhmetshin *et al*, *Phys. Lett.* B **364**, 199 (1995).
8. R.R. Akhmetshin *et al*, Preprint BudkerINP 95-62, Novosibirsk 1995.
9. G.V.Fedotovich(CMD-2 collaboration), Proceedings of the "Workshop on Physics and Detectors for DAFNE'95", Frascati, April 4-7,1995,p.571.
10. L.Montanet *et al*, *Phys. Rev.* D **54**, 341 (1996).
11. N.N.Achasov, V.Gubin and E.P.Solodov, hep-ph 9610282.
12. A. Lysenko *et al*, *Nucl. Instrum. Methods* A **359**, 419 (1995).

PERTURBATIVE CORRECTIONS TO THE HEAVY BARYON QCD SUM RULES

O.I.YAKOVLEV

Institut für Physik, Johannes-Gutenberg-Universität, Staudinger Weg 7, D-55099 Mainz, Germany

Budker Institute of Nuclear Physics (BINP), pr. Lavrenteva 11, Novosibirsk, 630090, Russia

We discuss an application of QCD sum rules to the heavy baryons Λ_Q and Σ_Q. The predictions for the masses of heavy baryons, residues and Isgur-Wise function are presented. The new results on two loop anomalous dimensions of baryonic currents and QCD radiative corrections (two- and three- loop contributions) to the first two Wilson coefficients in OPE are explicitly presented.

1 Introduction

Baryons with one b quark are very nice systems for application of Heavy Quark Effective Theory (HQET)[1]. It allows one to organize the determination of the properties of baryons in an $1/m_Q$-expansion, the leading term of which gives rise to the spin-flavour symmetry. Well known predictions of the HQET are the relations between different hadron transition form factors. For example, the six form-factors describing the $\Lambda_b \to \Lambda_c$ electro-weak transitions are reduced to one universal Isgur-Wise function $\xi(v \cdot v')$ in the HQ limit [2,3,4]. However, one still remains with many non-perturbative parameters, such as the mass of the baryon, the Isgur-Wise function and the averaged kinetic and magnetic energy of the baryon, which should be estimated by using some non-perturbative method as sum rules[5], lattice calculation or some potential model. In the present paper we review an application of the QCD sum rule method to calculate the masses, residues of heavy baryons and baryonic Isgur-Wise function[11,12,13,14,15,16,17,18,19,20,22,23,24].

2 Currents, anomalous dimensions and residues

For each of the ground state baryon currents there are two independent current components J_1 and J_2:

$$\begin{aligned} J_{\Lambda 1} &= [q^{iT} C\tau\gamma_5 q^j] Q^k \varepsilon_{ijk}, \\ J_{\Lambda 2} &= [q^{iT} C\tau\gamma_5\gamma_0 q^j] Q^k \varepsilon_{ijk}, \\ J_{\Sigma 1} &= [q^{iT} C\tau\vec{\gamma} q^j] \cdot \vec{\gamma}\gamma_5 Q^k \varepsilon_{ijk}, \\ J_{\Sigma 2} &= [q^{iT} C\tau\gamma_0\vec{\gamma} q^j] \cdot \vec{\gamma}\gamma_5 Q^k \epsilon_{ijk}. \end{aligned} \quad (1)$$

The anomalous dimensions of the heavy baryon currents up to second order was calculated recently in [22] and read (for example in the MS scheme with naively anticommuting γ_5, $a = \frac{\alpha_s}{4\pi}$, $k = 16\zeta(2)$)

$$\gamma_{\Lambda 1} = -8a + \frac{1}{9}(k + 40N_F - 796)a^2, \quad (2)$$

$$\gamma_{\Lambda 2} = -4a + \frac{1}{9}(k + 20N_F - 322)a^2, \quad (3)$$

$$\gamma_{\Sigma 1} = -4a + \frac{1}{9}(k + 20N_F - 290)a^2, \quad (4)$$

$$\gamma_{\Sigma 2} = -\frac{8}{3}a + \frac{1}{27}(3k + 8N_F + 324)a^2. \quad (5)$$

The anomalous dimensions are ingredient of renormalization group invariant sum rules. Numerically effects of γ_2 are very small and gives about $1-2\%$ corrections to the current redefinition.

Let us define residues $F_i(\mu)$ $(i = \Lambda, \Sigma)$ of the baryonic currents according to

$$\langle 0|J(\mu)|\Lambda_Q\rangle = F_\Lambda(\mu)u, \ \langle 0|J(\mu)|\Sigma_Q\rangle = F_\Sigma(\mu)u, \quad (6)$$

where u is spinor.

3 Correlator of two baryonic currents

In order to obtain information about the value of the mass of the baryon and its residue one considers the correlator of two baryonic currents

$$\Pi(\omega = k \cdot v) = i \int d^4x e^{ikx} \langle 0|TJ(x)\bar{J}(0)|0\rangle, \quad (7)$$

where k_μ and v_μ are the residual momentum and four velocity in $p_\mu = m_Q v_\mu + k_\mu$, respectively. $P(\omega)$ can be factorized into a spinor dependent piece and scalar function $P(\omega)$ according to

$$\Pi(\omega) = \Gamma' \frac{1 + \not{v}}{2} \bar{\Gamma}' \frac{1}{4} \mathrm{Tr}(\Gamma\bar{\Gamma}) 2\,\mathrm{Tr}(\tau\bar{\tau}) P(\omega). \quad (8)$$

The correlator function $P_{\rm OPE}(\omega)$ satisfies the dispersion relation

$$P_{\rm OPE}(\omega) = \int_0^\infty \frac{\rho(\omega')d\omega'}{\omega' - \omega - i0} + \text{subtraction}, \quad (9)$$

where $\rho(\omega) = Im(P(\omega))/\pi$ is the spectral density. The leading perterbative term and the next-to-leading term in OPE (gluon condensate contribution) give the spectral densities

$$\rho_0(\omega) = \frac{\omega^5}{20\pi^4}, \quad \rho_4(\omega) = c\frac{\alpha_s\langle GG\rangle}{32\pi^3}\omega. \quad (10)$$

Next we consider the radiative corrections to the spectral density of the perturbative contribution. There are four different three loop graphs contributing to the correlator, which are shown in Fig. 1 in Ref.[24]. The fact that all graphs in Fig. 1 have two-point two-loop subgraphs greatly simplifies the calculational task. One can first evaluate the respective subgraphs which leaves one with a one-loop integration. The first two-loop integration can be performed by using algebraic method described in [21]. It is important to note that the results of the two-loop integration are polynomials of the external momentum relative to this subgraph. Hence, the last integration is really a one-loop one, but the power of one of the propagators becomes a non-integer number. The evaluation of results in a Taylor expansion in $1/\epsilon$ gives [24] (with $x = \left(\frac{-2\omega}{\mu}\right)^{-2\epsilon}$)

$$P(\omega) = -\frac{32\omega^5}{(4\pi)^4}\left[x^2\frac{1}{40}\left(\frac{1}{\epsilon} + \frac{107}{15}\right) + \frac{\alpha_S}{4\pi}x^3 \cdot \left(\frac{n^2-4n+6}{45\epsilon^2} + \frac{40\zeta(2)+61n^2-234n+396}{225\epsilon}\right)\right]. \quad (11)$$

Here we assume that matrix Γ_1 in Eq.(1) is an antisymmetrized product of n Dirac matrices: $\Gamma = \gamma^{[\mu_1}\cdots\gamma^{\mu_n]}$. This introduces a n- and s-dependence in the QCD corrections due to the identities

$$\gamma_\alpha\Gamma\gamma_\alpha = h\Gamma = (-1)^n(D-2n)\Gamma, \ \gamma_0\Gamma\gamma_0 = (-1)^n s\Gamma. \quad (12)$$

The correlator is renormalized by the renormalization factor of the baryonic current, which is derived in [14],

$$P(\omega) = Z_J^2 P^{\rm ren}(\omega) \quad Z_J = 1 + \frac{\alpha_S C_B}{4\pi\epsilon}(n^2-4n+6). \quad (13)$$

The multiplication with Z_J^2 results in the cancelation of the second power in $1/\epsilon$. The first power in $1/\epsilon$ is purely real and hence does not contribute to the spectral density. The renormalized spectral density $\rho^{\rm ren}(\omega) = Im(P^{\rm ren}(\omega))/\pi$ must in fact be finite and can be read immediately off Eq. (11),

$$\rho^{\rm ren}(\omega) = \rho_0(\omega)\left[1 + \frac{\alpha_S}{\pi}r(\omega/\mu)\right], \quad \text{where}$$

$$\rho_0(\omega) = \frac{\omega^5}{20\pi^4} \quad \text{and}$$

$$r(\omega/\mu) = \frac{2}{3}(n^2-4n+6)\ln\left(\frac{\mu}{2\omega}\right) + \frac{2}{45}(60\zeta(2)+38n^2-137n+273). \quad (14)$$

The α_S correction can be seen to depend on the properties of the light-side Dirac matrix in the heavy baryon current. The results in the naively anticommuting γ_5-scheme (AC) are

$$r_{\Lambda 1}(\omega/\mu) = 4\ln\left(\frac{\mu}{2\omega}\right) + \underbrace{\frac{2(20\zeta(2)+91)}{15}}_{\approx 16.51}, \quad (15)$$

$$r_{\Lambda 2,\Sigma 1}(\omega/\mu) = 2\ln\left(\frac{\mu}{2\omega}\right) + \underbrace{\frac{4(10\zeta(2)+29)}{15}}_{\approx 12.12},$$

$$r_{\Sigma 2}(\omega/\mu) = \frac{2}{3}ln\left(\frac{\mu}{2\omega}\right) + \underbrace{\frac{2(60\zeta(2)+151)}{45}}_{\approx 11.10}.$$

The coefficient of the logarithmic term $\ln(2\omega/\mu)$ in Eq. (14) coincides with twice the one-loop anomalous dimension given in Eq. (13), as expected. The results for the Baryons Λ_1 and Λ_2 in the 't Hooft-Veltman γ_5-scheme (HV) differ from those presented above. But we know that currents in different schemes should be connected by finite renormalization factors Z, $J_{AC} = ZJ_{HV}$. Such factors was recently derived from two-loop anomalous dimensions of baryonic currents [22]. They read

$$Z_{\Lambda 1} = 1 - \frac{4\alpha_S}{3\pi} \quad \text{and} \quad Z_{\Lambda 2} = 1 - \frac{2\alpha_S}{3\pi}. \quad (16)$$

By multiplying the results in the 't Hooft-Veltman scheme by Z^2 we obtain the same results as in the naively anticommuting γ_5-scheme.

The results show that the α_S-corrections amount to about 100%, which makes perturbative QCD radiative "corrections" very important in QCD sum rules. We used $\mu = 2\omega \approx 1\ GeV$ and $\alpha_S(\mu) = 0.3$.

4 Contribution of quark condensate

Next, we consider the contribution of the quark condensate, which appears in the nondiagonal sum rules. The leading and next-to-leading spectral density are

$$\rho(\omega) = -\frac{\langle\bar{q}q\rangle}{\pi^2}\omega^2 \;\; \rho_5(\omega) = 2\Big(1-\frac{c}{2}\Big)\frac{\langle\bar{q}q\rangle m_0^2}{16\pi^2}. \quad (17)$$

The radiative corrections to the quark condensate term can be quite important, and we take it into account. There are 8 different graphs contributing to the correlator, which are shown in Fig. 2 in Ref.[24]. We used the same method as we used for the perturbative term. For the renormalized spectral density we get

$$\rho^{\rm ren}(\omega) = -\frac{\langle\bar{q}q\rangle^{\rm ren}\omega^2}{\pi^2}\Big[1 + \\ +\frac{\alpha_s}{4\pi}\Big(\frac{4}{3}(2n^2-8n+7+2(n-2)s)\cdot\ln\Big(\frac{\mu}{2\omega}\Big) + \\ +\frac{2}{3}(8n^2-28n+37+8ns-14s+8\zeta(2))\Big)\Big]. \quad (18)$$

Then we proceed with the usual QCD sum rules analysis and equate the theoretical result for $P_{\rm OPE}(\omega)$ with the dispersion integral over the hadron states saturated by the lowest lying state with the bound state energy E_R plus exited states and continuum. So the phenomenological part of the sum rule is given by the spectral density $\rho_{\rm ph}(\omega) = \rho_{\rm res}(\omega) + \rho_{\rm cont}(\omega)$, where the contribution $\rho_{\rm res}$ of the low-lying baryon state is $\rho_{\rm res}(\omega) = \frac{|F|^2}{2}\delta(\omega - E_R)$. As is usual for the contribution of excited states and continuum contributions we assume hadron-parton duality and take $\rho_{\rm cont}(\omega) = \theta(\omega - E_C)\rho(\omega)$, where ρ is the result of the OPE calculations.

5 Numerical results

Let us discuss the sum rule analysis. First, we analyse the dependence of the bound state energy E_R as a function of the energy of continuum E_C and the Borel parameter T in a wide region of these arguments and try to find regions of stability in T and E_c. Second, we fix the energy of continuum $E_c = E_c^{\rm best}$ by requiring that $E_R(T)$ should have the highest possible stability in its dependence on the Borel parameter T. We take into account the α_S-correction to the spectral density and obtain

$$E_\Lambda = 0.9 \pm 0.2\, GeV \text{ and } E_C^{\rm best} = 1.2 \pm 0.2\, GeV. \quad (19)$$

The analysis of sum rules at $E_\Lambda = 0.9\, GeV$ gives for the Λ-residue

$$F_\Lambda = (0.03-0.04)\, GeV^3 \text{ and } E_C = 1.0-1.4\, GeV. \quad (20)$$

All other results are summarized in the Table 1 , where we compare our results with the leading order results obtained in the [14,17,19] and some experimental values.

6 The Isgur-Wise function

Next, we consider semileptonic transition $\Lambda_b \to \Lambda_c$. The matrix elements of the weak current for $\Lambda_b \to \Lambda_c$ at the leading order $1/m_Q$ are determined only by Isgur-Wise function

$$< \Lambda_c|\bar{c}\Gamma b|\Lambda_b >= \xi(y)\bar{u}_c\Gamma u_b. \quad (21)$$

where $y = v_b \cdot v_c$ and Γ is some gamma matrix. The Isgur-Wise function was calculated in Ref.[15] by using three-point QCD sum rules. The slope of Isgur-Wise function at y=1 is

$$\rho^2 = -1.15 \pm 0.2. \quad (22)$$

The uncertainty is connected mainly with an assumption about continuum model. We have found that the shape of the Isgur-Wise function nearly coincides with the ansatz formula

$$\xi(y) = \frac{2}{y+1}exp[(2\rho^2-1)\frac{y-1}{y+1}], \quad (23)$$

with the slope in Eq.(22). $1/m_Q$ corections to $\Lambda_b \to \Lambda_c$ transition were discussed recently in [20]. The important $1/m_Q$ effects to the decay come only from the weak current expansion.

7 Conclusions

We have calculated one and two-loop anomalous dimensions of baryonic currents. We have studied the expansion of the correlator of two heavy baryon currents at small Euclidian distances. The radiative corrections to the first two Wilson coefficients are calculated. The heavy baryons sum rules in α_S order are derived. The predictions for the mass, residues , the slope and shape of Isgur-Wise function are presented.

	14	17	19	L.O.	N.L.O.
$E_C(\Lambda)$	1.20	1.2 ± 0.1	1.20 ± 0.15	1.2 ± 0.2	1.2 ± 0.2
$E_C(\Sigma)$	1.46	1.4 ± 0.1	1.30 ± 0.15	1.4 ± 0.2	1.4 ± 0.2
$E_R(\Lambda)$	0.78	0.9 ± 0.1	0.79 ± 0.05	0.8 ± 0.2	0.92 ± 0.2
$E_R(\Sigma)$	0.99		0.96 ± 0.05	1.02 ± 0.2	1.12 ± 0.2
Diff.	0.21		0.17	0.22	0.2
F_Λ	2.3 ± 0.5	2.5 ± 0.5	1.7 ± 0.6	2.4 ± 0.5	3.2 ± 0.5
F_Σ	3.5 ± 0.6	4.0 ± 0.5	4.1 ± 0.6	3.4 ± 0.5	5.2 ± 0.5

Table 1: All energies like E_C, E_R are given in GeV, the residues in $10^{-2}\, GeV^3$. The value of the Borel parameter is $T = 0.6\, GeV$.

Acknowledgments

This work was partially supported by the BMBF, FRG, under contract 06MZ566, and by the Human Capital and Mobility program under contract CHRX-CT94-0579. I would like to thank A.G. Grozin, J.G. Körner and S.Groote for the interesting collaboration.

References

1. See for example: M.Neubert *Phys. Rep.* **245**, 259 (1994).
2. H.Georgi, *Nucl. Phys.* B **363**, 301 (1991).
3. T.Mannel, W.Roberts, Z.Ryzak, *Nucl. Phys.* B **355**, 38 (1991).
4. F.Hussein, J.G.Körner, M.Krämer and G.Thompson, *Z. Phys.* C **51**, 321 (1991).
5. M.A.Shifman, A.I.Vainstein and V.I.Zakharov, *Nucl. Phys.* B **147**, 385 (1979); *Nucl. Phys.* B **147**, 488 (1979).
6. B.L.Ioffe, *Nucl. Phys.* B **188**, 317 (1981); Errata **B191** 591 (1981).
7. V.M.Belyaev and B.L.Ioffe, Sov. Phys. JETP **56** 493 (1982).
8. Y.Chung, H.G.Dosch, M.Kremer and P.Schall, *Nucl. Phys.* B **197**, 55 (1981).
9. A.A.Pivovarov and L.R.Surguladze, *Nucl. Phys.* B **360**, 97 (1991).
10. A.A.Ovchinnikov, A.A.Pivovarov and L.R.Surguladze, Int. J. Mod. Phys. **A6** 2025 (1991).
11. E.V.Shuryak, *Nucl. Phys.* B **198**, 83 (1982).
12. B.Y.Block and V.L.Eletsky, *Z. Phys.* C **30**, 151 (1986); *Z. Phys.* C **30**, 229 (1986).
13. E.Bagan, M.Chabab, H.G.Dosch and S.Narison, *Phys. Lett.* B **278**, 367 (1992); *Phys. Lett.* B **287**, 176 (1992).
14. A.G.Grozin and O.I.Yakovlev, *Phys. Lett.* B **285**, 254 (1992).
15. A.G.Grozin and O.I.Yakovlev, *Phys. Lett.* B **291**, 441 (1992).
16. E.Bagan, M.Chabab, H.G.Dosch and S.Narison, *Phys. Lett.* B **301**, 243 (1993).
17. P. Colangelo, C.A. Dominguez, G. Nardulli and N. Paver, *Phys. Rev.* D **54**, 4622 (1996)
18. P.Colangelo and F.De Fazio, BARI-TH/95-230, hep-ph/9604425.
19. Y.B.Dai, C.S.Huang, C.Liu and C.D.Lü, *Phys. Lett.* B **371**, 99 (1996).
20. Y.B. Dai, C.S. Huang, M. Huang, C. Liu, hep-ph/9608277.
21. D. Brodhurst and A.G. Grozin, *Phys. Lett.* B **267**, 105 (1991).
22. S. Groote, J.G. Körner and O.I. Yakovlev, *Phys. Rev.* D **54**, 3447 (1996).
23. S. Groote, J.G. Körner and O.I. Yakovlev, Mainz Preprint MZ/TH-96-21, hep-ph/960469.
24. S. Groote, J.G. Körner and O.I. Yakovlev, (in preparation) , MZ/TH-96-31, will be published.
25. S. Capstick and N. Isgur, *Phys. Rev.* D **34**, 2809 (1986).
26. UA1 Collab., C. Aldajar et al., CERN PPE/91-202 (1991).